

# Results of coherent backscatter radar imaging using Capon's method and measurements made by the Sao Luis radar interferometer

Gebreab K. Zewdie and Fabiano S. Rodrigues  
The University of Texas at Dallas,  
William B. Hanson Center for Space Sciences  
Richardson, TX, USA

**Abstract**—Interferometric radar imaging of F-region spread F irregularities is used to determine the distribution of scatterers within the radar field of view. In this study, we investigate the use of the Capon's spectral method for estimating the distribution of equatorial spread F (ESF) irregularity structures observed by a small, low power coherent backscatter radar interferometer located at the equatorial site of Sao Luis ( $2.59^{\circ}S, 44.21^{\circ}W, -2.35^{\circ}$  dip.), Brazil. To evaluate the performance of the method, we show numerical simulations for typical F-region measurement conditions. Results for the Fourier imaging method are also shown for comparison. The simulation shows that, despite the short baselines of the Sao Luis radar, the Capon technique is capable of distinguishing features with km scale sizes (in the zonal direction) at F-region heights. We also investigated the application of the Capon algorithm to actual measurements made by the Sao Luis radar, and obtained high resolution images of equatorial spread F (ESF) scattering structures. In this presentation, we will show results of the Capon images during different types of equatorial spread F events, and will compare the results with images obtained using the conventional Fourier method. As predicted by the numerical simulations, we are able to distinguish features of the scattering structures with resolution of a few km in the zonal direction. We have been able, in particular, to identify the morphology of scattering structures during bottom-type layers. Signatures of underlying deca-kilometric waves, similar to those observed by [3] and [7] were detected. The observations suggest the action of the so-called collisional shear instability.

## I. INTRODUCTION

Equatorial spread F (ESF) refers to a wide range of electron density irregularities occurring in the equatorial F-region ionosphere. ESF is associated with interchange plasma instabilities, which can create larger scale size plasma density perturbations. Secondary plasma instabilities then create smaller scale irregularities [8]. In addition to the scientific aspect of studying instabilities in space plasmas, investigation of ESF is also motivated by its impact on the propagation of trans-ionospheric radio waves such as those used for remote sensing, navigation, and communication [4].

Coherent scatter radars (CSR) have greatly helped our understanding of ESF. Conventional radar measurements are capable of providing information about the range of irregularities, as a function of time, as well as the mean phase velocity of the irregularities producing the echoes. Using interferometric techniques, one can estimate the distribution of the scatterers

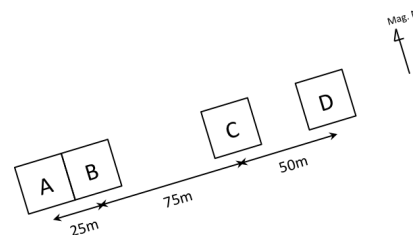


Fig. 1. Diagram showing the distribution of the antenna sets used for the interferometric observations. Each antenna set is formed by a  $4 \times 4$  array of Yagi antennas. A, B, C and D represent the antenna sets. Transmissions are made with sets A and B. Reception is made with all of the antenna sets. The magnetic declination is approximately  $21^{\circ}$ .

responsible for the observed echoes. Using measurements made by multiple antenna baselines at Jicamarca, [5] obtained the first in-beam interferometric images of equatorial electrojet irregularities.

In this paper, we present the application of the Capon's spectral method, [6], for estimating the distribution of ESF irregularity structures using measurements made by a small, low power CSR interferometer located at the equatorial site of Sao Luis ( $2.59^{\circ}S, 44.21^{\circ}W, -2.35^{\circ}$  dip.), Brazil. The radar consists of four antenna baselines, the longest baseline having 150 m length. Description of the radar can be found in [2].

## II. MEASUREMENTS

The measurements available for this study were made by a 30 MHz CSR interferometer. The radar is equipped with four independent antenna sets connected to four receivers. Each antenna set is formed by an array of  $4 \times 4$  Yagi antennas. The arrays have been placed non-uniformly in the magnetic zonal direction for radar imaging studies of scattering layers. Figure 1 shows the distribution of the antennas in the magnetic zonal direction.

For F-region measurements, we used 28-bit coded pulses, with a 9.33 ms inter-pulse period (IPP). The baud length and sampling were 2.5 km. A total of 250 samples were collected per IPP. This observation setup allowed us to make measurements of the F-region from 200 to 825 km altitude with a range resolution 2.5 km.

### III. ANALYSIS AND RESULTS

In-beam CSR imaging techniques are used to determine the distribution of scatterers as a function of height and zenith angle ( $\psi$ ). The real-valued, continuous function representing this distribution is referred to as Brightness distribution  $B(\psi)$ , and it is computed for each range gate. The brightness distribution is closely related to the cross-correlation of scattered signals (called visibility) received by antennas spaced by a distance  $d$ . A commonly used estimator for the normalized cross-correlation of signals measured by spaced antennas 1 and 2 is given by:

$$\rho_{12} = \frac{\langle V_1 V_2^* \rangle}{\sqrt{(\langle |V_1|^2 \rangle - N_1)(\langle |V_2|^2 \rangle - N_2)}} \quad (1)$$

The angle brackets represent an ensemble average.  $V_1$  and  $V_2$  are the complex-valued voltage samples measured by antennas 1 and 2, respectively.  $N_1$  and  $N_2$  are estimates of the noise power in each antenna.

Considering the practical case of a finite number ( $M$ ) of visibility measurements, the Fourier based estimate of the brightness distribution ( $\hat{B}$ ) can be obtained in [6] and is given as:

$$\hat{B}(\psi) = \mathbf{w}^H \mathbf{V} \mathbf{w} \quad (2)$$

Where  $H$  denotes the Hermitian operator. For  $n$  non-redundant baselines,  $\mathbf{V}$  is the  $n \times n$  visibility matrix, and  $\mathbf{w}$  is the weight vector that has the following form [6]:

$$\mathbf{w} = [e^{jk \cdot d_1} \quad e^{jk \cdot d_2} \quad \dots \quad e^{jk \cdot d_n}]^T \quad (3)$$

Unlike the conventional Fourier transform, the Capon method, [1], is based on constrained optimization problem to obtain a set of weights ( $\mathbf{w}_C$ ) that will not only provide a high resolution spectrum but will also suppress the effects of interfering signals. The Capon weights lead to an estimate of the brightness function given by: [6]

$$\hat{B}(\mathbf{k}) = \frac{1}{\mathbf{w}^H \mathbf{V}^{-1} \mathbf{w}} \quad (4)$$

The top panel of Figure 2 shows the range-time-intensity (RTI) maps of the echoes observed on March 14, 2006. The RTI map shows bottom-type irregularities starting around 23:30 UT (20:30 LT) at approximately 250 km altitude. The layer lasts for about 2 hours and gains altitude, reaching approximately 350 km around 01:25 UT on March 15. Topside irregularities start to be observed around 01:25 UT, with echoes reaching as high as 700 km altitude.

The bottom panels of Figure 2 show the in-beam images produced by our algorithms for measurements made at 01:27 UT. The left panel shows the image produced by the Fourier method, while the right panel shows the image produced by the Capon method. Both images show the passage of a small plume that drifts from west (right hand side) to the east. The images also show that the structure is tilted to the west and this is, presumably, caused by height variations in the zonal plasma drifts. More importantly, one can see that the

Capon method produces a sharper, more detailed image than the Fourier method. For instance, the Capon image shows the scattering region is much narrower (in the zonal direction) than what is presented by the Fourier image. The Fourier image shows scattering features that are much broader and diffuse, which is a direct result of the short baselines used for visibility functions.

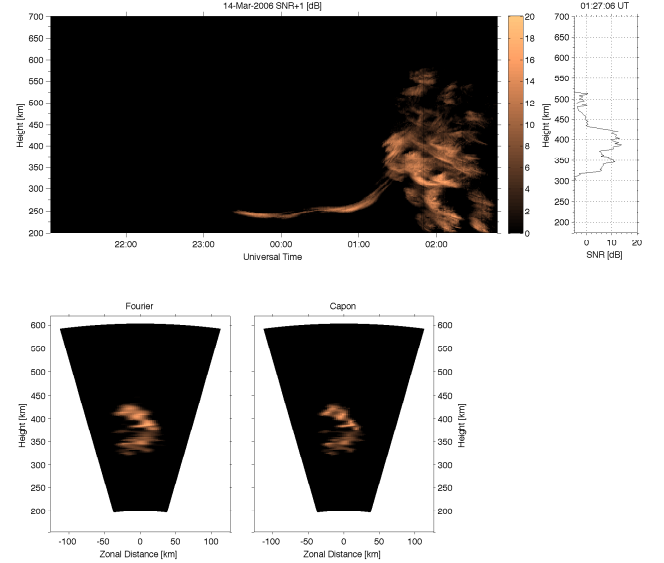


Fig. 2. The top panel shows the Range-Time-Intensity map of F-region observations made by the Sao Luis radar. The bottom panels show the images obtained with the Fourier Transform (left) and Capon methods (right) for observations around March 15 2006 at 01:27 UT (UT = LT + 3)

### REFERENCES

- [1] Capon, J., (1969), High-Resolution Frequency- Wavenumber Spectrum Analysis, *IEEE Proceeding*, 57, 1408-1418.
- [2] de Paula, E., and D. L. Hysell, (2004), The Sao Luis 30 MHz coherent scatter ionospheric radar: System description and initial results, *Radio Science*, 39, 2004.
- [3] Hysell, D. L. , J. Chun , and J. L. Chau,(2004), Bottom-type scattering layers and equatorial spread F, *Annales Geophysicae*, 22: 40614069
- [4] Kintner, P. M., B. M. Ledvina, and E. R. de Paula (2007), GPS and ionospheric scintillations, *Space Weather*,
- [5] Kudeki, E., and F. Surucu (1991), Radar Interferometric Imaging of field aligned Plasma Irregularities in the Equatorial Electrojet, *Geophys. Res. Lett.* 18, 41-44. *Radio Science*, 39, 2004.
- [6] Palmer, Robert D., Sridhar Gopalram, and Tian- You Yu (1998), Coherent radar imaging using Capon's Method, *Radio Science*, 33, 1585-1598.
- [7] Rodrigues, F.S., D.L. Hysell, and E. R. de Paul (2008), Coherent backscatter radar imaing in Brazil: large-scale waves in the bottomside F-region at the onset of equatorial spread F, *Ann. Geophys.*, 26, 3355-3364.
- [8] Woodman, R. F., (2009), Spread F- an old equatorial aeronomy problem finally resolved?, *Ann. Geophys.*, 27, 1915-1934.